

# Asymmetrically Functionalized Graphene for Photodependent Diode Rectifying Behavior\*\*

Dingshan Yu, Enoch Nagelli, Rajesh Naik, and Liming Dai\*

As an atomically thin sheet of carbon atoms packed in a two-dimensional (2D) honeycomb lattice with excellent electronic, thermal, and mechanical properties, graphene has shown great potential for a wide range of applications. Examples include the use of graphene and its derivatives as transparent conductive electrodes or active materials in solar cells, counter electrodes in dye-sensitized solar cells, electrocatalysts for oxygen reduction in fuel cells, high-performance electrodes in supercapacitors, batteries, actuators, and sensors.<sup>[1,2]</sup> Of particular interest, Guo et al.<sup>[2f]</sup> reported a significant advancement in the development of layered graphene/quantum dots for highly efficient solar cells. Stoller et al.<sup>[1j]</sup> produced graphene-based supercapacitors free from any conducting filler with a specific capacitance of 135 F g<sup>-1</sup> in aqueous electrolytes. We also demonstrated that N-doped graphene could act as a metal-free electrode with a much better electrocatalytic activity, long-term operational stability, and tolerance to crossover effect than platinum for oxygen reduction in alkaline fuel cells.<sup>[2b]</sup> By using graphene as a superior dimensionally compatible and electrically conductive component, Guo et al.<sup>[2g,h]</sup> further constructed a smart graphene-based multifunctional biointerface for cell growth as well as in situ selective and quantitative molecular detection. There is now a pressing need to integrate graphene sheets into multidimensional and multifunctional systems with spatially well-defined configurations, and hence integrated systems with a controllable structure and predictable performance. This requires controlled functionalization of graphene sheets at the molecular level, which is still a big challenge.

The recent availability of solution-processable graphene by exfoliation of graphite into graphene oxides (GOs), followed by solution reduction,<sup>[3]</sup> has allowed the functionalization of graphene sheets through various solution reactions.<sup>[4]</sup> As far as we are aware, however, there is still no report on the asymmetric functionalization of graphene sheets by attaching different chemical moieties to their two opposite surfaces. The asymmetric functionalization, if realized, should significantly advance the self-assembling of graphene sheets into many new multidimensional and multifunctional systems with molecular-level control. Herein, we report for the first time a simple but effective asymmetric modification method for functionalizing the two opposite surfaces of individual graphene sheets with different nanoparticles (NPs) in either a patterned or nonpatterned fashion. The resultant asymmetrically modified graphene sheets with ZnO and Au NPs on their two opposite surfaces were demonstrated to show a strong photodependent diode rectifying behavior.

We have previously developed a polymer masking technique for asymmetric functionalization of carbon-nanotube sidewalls by sequentially masking vertically aligned carbon nanotubes twice, with only half of the nanotube length being modified each time.<sup>[5,6]</sup> In the present study, we used a new polymer masking technique for sequentially masking individual graphene sheets twice with only one side of the surface being modified each time. In a typical experiment, an aqueous dispersion of chemically derived graphene sheets was firstly prepared by the method described in the literature.<sup>[3c]</sup> We then deposited a dilute aqueous solution (0.05 mg mL<sup>-1</sup>) of the well-dispersed graphene nanosheets (Figure 1a and Figures S1 and S2 in the Supporting Information) onto a silicon substrate by spin-coating (900 rpm, Spin Coater KW-4A, Chemat Technology). Individual graphene sheets on the substrate were then treated by an acetic acid plasma<sup>[6b,c]</sup> to introduce carboxylic groups on the exposed surface of each of the silicon-supported graphene sheets (Figure 2a), while their opposite surface was protected by the silicon substrate to be free from the plasma treatment.

Thereafter, spherical ZnO NPs (ca. 10 nm in diameter, Figure 1b and Figure S3 in the Supporting Information) were attached to the plasma-treated graphene surface (Figures 1c and 2b) through the specific interaction of carboxylic groups with oxide particles according to previously published procedures.<sup>[7]</sup> This was followed by spin-coating (2000 rpm, Spin Coater KW-4A, Chemat Technology) a thin layer of poly(methyl methacrylate) (PMMA) from a CHCl<sub>3</sub> solution (10 wt % PMMA) to mask the ZnO-attached graphene surface (Figure 2c). The PMMA-coated, ZnO-attached graphene sheets were then separated from the silicon substrate by immersion in a HF aqueous solution<sup>[6]</sup> (ca. 5 wt %) to

[\*] Dr. D. Yu, E. Nagelli, Prof. L. Dai  
 Department of Macromolecular Science and Engineering and  
 Department of Chemical Engineering  
 Case Western Reserve University  
 10900 Euclid Avenue, Cleveland, OH 44106 (USA)  
 and  
 Interdisciplinary School of Green Energy  
 Ulsan National Institute of Science and Technology (UNIST)  
 Ulsan 689-798 (South Korea)  
 Fax: (+1) 216-368-3016  
 E-mail: liming.dai@case.edu  
 Dr. R. Naik  
 Materials and Manufacturing Directorate  
 Air Force Research Laboratory  
 Wright-Patterson AFB, OH 45433 (USA)

[\*\*] This work was supported financially by the NSF and AFRL/DAGSI (RX2-CWRU-10-1). Partial support from WCU-UNIST, AFOSR-NBIT, and NSFC is also acknowledged.

Supporting information for this article is available on the WWW under <http://dx.doi.org/10.1002/anie.201101305>.

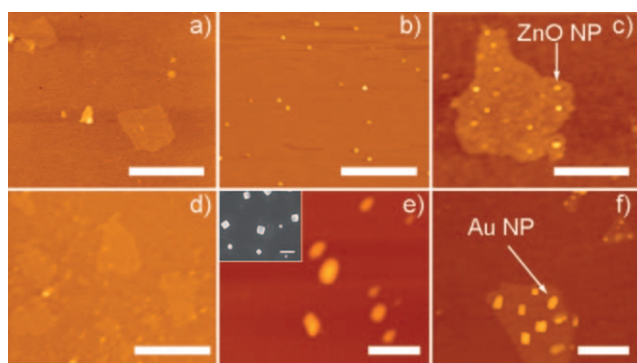


**Figure 1.** AFM images of a) graphene sheets, b) spherical ZnO NPs, c) a graphene surface with attached spherical ZnO NPs, d) a graphene sheet with the ZnO-attached surface coated by PMMA and the bare surface exposed, e) cubic Au NPs, and f) an asymmetrically modified graphene sheet with the Au-modified surface exposed. The inset of (e) shows an SEM image of the cubic Au NPs (see Figure S4 in the Supporting Information). Scale bars: a–c, f) 2  $\mu\text{m}$ ; d) 4  $\mu\text{m}$ ; e) 1  $\mu\text{m}$ ; inset of (e): 100 nm. Note that the images shown in (c) and (f) were not obtained from the same graphene sheet due to technical difficulties.

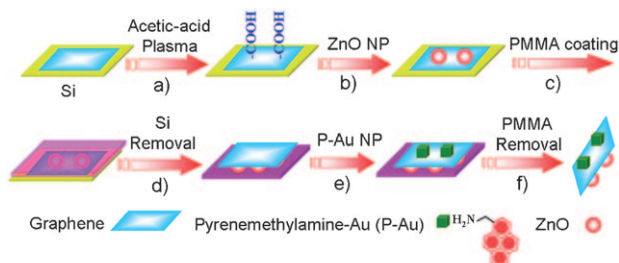


**Figure 2.** Steps for asymmetrical functionalization of the two opposite surfaces of individual graphene sheets with ZnO and Au NPs, respectively.

expose the bare surface of graphene (Figures 1 d and 2 d) for subsequent functionalization with cubic Au NPs (ca. 60 nm edge length, Figure 1 e and Figure S4 in the Supporting Information) grafted with 1-pyrenemethylamine for  $\pi$ - $\pi$  stacking<sup>[8]</sup> onto the bare graphene surface (Figures 1 f and 2 e). Subsequent removal of the PMMA supporting layer by ultrasonication in  $\text{CHCl}_3$  led to the release of the asymmetrically modified graphene sheets with the spherical ZnO and cubic Au NPs on their two opposite surfaces (Figure 2 f).

Among the many functional entities that can be asymmetrically attached to individual graphene sheets through the method shown in Figure 2, we chose ZnO and Au NPs of different sizes and shapes for easy characterization by direct “visualization” with microscopy techniques (e.g., atomic force microscopy (AFM) and scanning electron microscopy (SEM); Figure 1 and Figures S2–S4 in the Supporting Information) and for their unique optoelectronic properties. As expected, the AFM image of the resultant ZnO-attached graphene given in Figure 1 c clearly shows many spherical ZnO particles deposited on one side of the graphene sheet. In contrast, Figure 1 f reveals an asymmetrically modified graphene sheet with cubic Au NPs attached to one side of the sheet, while the ZnO-attached surface of the same graphene sheet was protected by the PMMA coating.

Further evidence for the asymmetric functionalization comes from scanning transmission electron microscopy (STEM) in conjunction with energy-dispersive X-ray (EDX) measurements. While the STEM image given in the inset of Figure 3 shows only the cubic Au NPs on one side of an

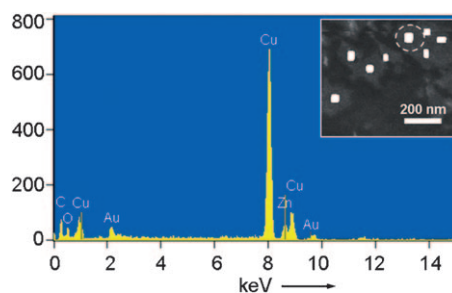


**Figure 3.** EDX spectrum of an asymmetrically modified graphene sheet with ZnO and Au NPs attached to two opposite surfaces. Inset: the corresponding STEM image (the EDX analysis area is indicated by a white circle). Note that the Cu signal comes from the copper TEM grid used in this study.

asymmetrically functionalized graphene sheet, the corresponding EDX spectrum (Figure 3) from the same side of the same graphene sheet reveals the presence of Zn and O signals in addition to those of Au and C. The Zn and O signals originate from the ZnO NPs attached to the graphene surface opposite to the Au NP-attached side, unambiguously indicating successful asymmetric functionalization.

Having successfully demonstrated the asymmetric modification of the two opposite surfaces of individual graphene sheets with different NPs in a nonpatterned fashion, we proceeded to explore the possibility of region-specific modification of the graphene surface with different NPs. As shown schematically in Figure 4 a, we also deposited a dilute aqueous solution ( $0.05 \text{ mg mL}^{-1}$ ) of the well-dispersed graphene nano-sheets<sup>[3c]</sup> onto a silicon substrate by spin-coating (see Figure 2). Individual graphene sheets on the substrate were then covered by PMMA micropatterns photolithographically produced according to a previously reported method<sup>[9]</sup> (see also the Supporting Information). Because of the random distribution of the graphene sheets on the substrate surface, one can anticipate that some graphene sheets may be partially masked by the PMMA micropatterns (step 1, Figure 4 a). Subsequent treatment with an acetic acid plasma allowed the attachment of ZnO NPs onto the PMMA-free graphene surface through the specific interaction between the plasma-induced carboxylic groups and oxide NPs (step 2, Figure 4 a),<sup>[7]</sup> as mentioned above. The concomitant deposition of ZnO NPs on the plasma-treated PMMA patterns cannot be ruled out, but they, if any, can be readily removed by dissolving the PMMA patterns in a  $\text{CHCl}_3$  solution (see the Supporting Information), thereby leading to graphene sheets with region-selectively attached ZnO NPs (Figure 4 b).

Furthermore, Au NPs prefunctionalized with 1-pyrenemethylamine could be selectively adsorbed onto the ZnO-deposited graphene surface in the ZnO-free regions

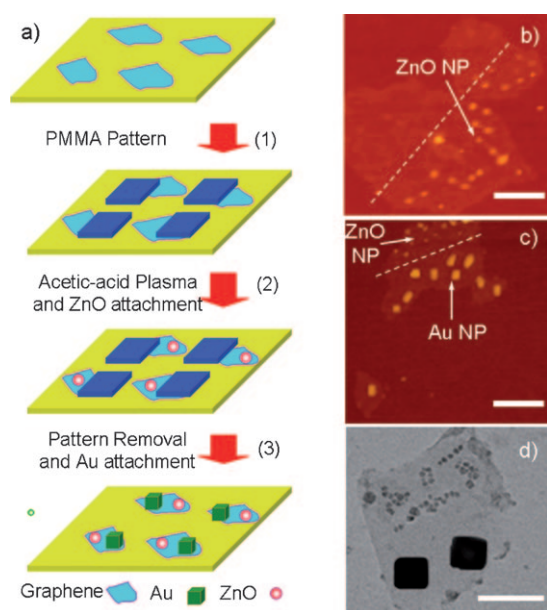


**Figure 4.** a) Patterned functionalization of graphene with spherical ZnO and cubic Au NPs (see the Supporting Information for the experimental details). b) AFM image of a modified graphene sheet with small spherical ZnO NPs region-specifically deposited on the plasma-treated area. c) AFM and d) TEM images of a graphene sheet modified with small spherical ZnO NPs deposited in the plasma-treated area and large cubic Au NPs attached in the ZnO/plasma-free region on the same graphene surface. Scale bars: b) 1  $\mu\text{m}$ ; c) 2  $\mu\text{m}$ ; d) 100 nm.

untreated by the plasma through the  $\pi$ - $\pi$  stacking interaction between the pyrene linkage and bare graphene surface (step 3, Figure 4a), as confirmed by Figure 4c. Possible deposition of Au NPs between the ZnO particles predeposited in the acetic acid plasma-treated region can be ruled out, as the plasma surface cannot support the  $\pi$ - $\pi$  stacking interaction with the pyrene linker.<sup>[10]</sup> This is further supported by the pattern of small spherical ZnO NPs with relatively large cubic Au NPs seen in the TEM image (Figure 4d), and the coexistence of Au, Zn, O, and C peaks in the corresponding EDX spectrum (Figure S9 in the Supporting Information). Besides, high-resolution TEM (HRTEM, Figure S10 in the Supporting Information) images of the region-selectively deposited ZnO and Au NPs clearly reveal their (100) lattice planes. Judicious application of the patterned surface modification and the asymmetric functionalization methods described above should lead to asymmetrically modified graphene sheets with different side/region-selectively attached functional moieties attractive for various device applications.

To demonstrate potential applications of the asymmetrically functionalized graphene sheets developed in this study, we used current-sensitive AFM<sup>[11]</sup> to test the electronic characteristics of the graphene sheet with ZnO and Au NPs attached to its opposite surfaces. As seen in Figure 5a, current-voltage ( $I$ - $V$ ) curves of the asymmetrically modified graphene sheet were measured by placing a gold-coated conducting AFM tip onto a ZnO NP with an applied voltage between the tip and Au-coated Si substrate, which is also in contact with the Au NPs attached to the graphene surface

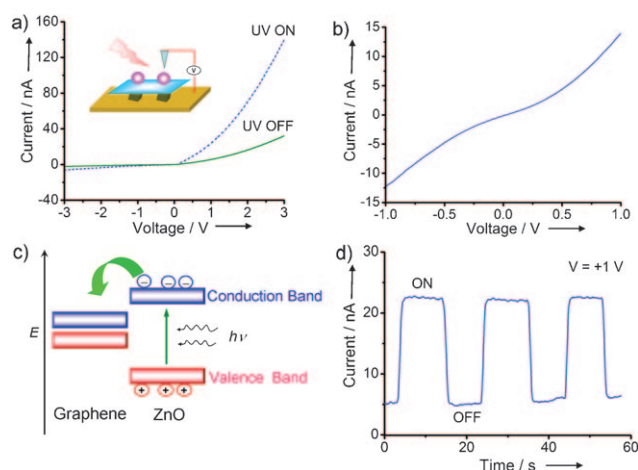


**Figure 5.** a)  $I$ - $V$  curves of the asymmetrically modified graphene with ZnO and Au NPs on its two opposite surfaces, with the AFM tip placed on a ZnO NP with and without UV illumination. Inset: contact configuration of the  $I$ - $V$  measurements. b)  $I$ - $V$  curve of the graphene/Au junction measured with the AFM tip placed on the ZnO-free region of the graphene surface. c) Energy band diagram for the graphene/ZnO junction. d) Photoresponse to UV light measured at  $V = +1$  V as a function of time.

facing down. Figure 5a shows the typical  $I$ - $V$  curves for the asymmetrically modified graphene (ZnO/graphene/Au) with and without UV illumination (Hg lamp, 4 W, and 366 nm). Clearly, the ZnO/graphene/Au junction acts as a diode and exhibits distinct rectifying characteristics at room temperature, whereas the  $I$ - $V$  curve of the graphene/Au junction measured with the AFM tip placed on the ZnO-free region on the graphene surface is nearly symmetrical and does not exhibit any obvious diode effect (Figure 5b).

Generally speaking, ZnO NPs are n-type semiconductors because of the presence of intrinsic defects such as oxygen vacancies,<sup>[12]</sup> and chemically derived (e.g., hydrazine reduction) few-layer graphene sheets exhibit p-type semiconducting behavior.<sup>[1e,13]</sup> The diodelike behavior observed above, therefore, arises mainly from the graphene/ZnO p-n junction.<sup>[14]</sup> As a control, we also tested the electronic properties of the ZnO/graphene junction (Figure S11 in the Supporting Information), which did indeed show a similar rectifying behavior.

More interestingly, it was found that the conductivity of the ZnO/graphene/Au junction could be significantly enhanced upon UV irradiation. With an applied bias of 2.0 V, the rectification ratio of the diode increased from 11 to 21 upon UV exposure (the rectification ratio is defined as the ratio of the forward current to the reverse current at  $\pm 2$  V), presumably as a result of the direct photocurrent injection from the n-type ZnO NPs into the p-type graphene sheet.<sup>[2f]</sup> Given that the work function and band gap of n-type ZnO are about 4.5 and 3.3 eV, respectively (the conduction band edge is about 4.1 eV),<sup>[15]</sup> and the chemically derived graphene sheet has a work function of around 4.4 eV<sup>[2f]</sup> with an energy gap of 10–50 meV,<sup>[16]</sup> a schematic energy band diagram is given in Figure 5c for the photoinduced mechanism. The photocurrent enhancement was found to be reversible and reproducible.

cible even in the ambient atmosphere. The photoresponse to UV light measured at  $V = +1$  V is plotted as a function of time in Figure 5d. Clear optical switching behavior with an on/off ratio of about 5 was demonstrated. As expected, no photocurrent generation was observed for the corresponding graphene/Au junction. Although further study is needed to understand the detailed charge-injection mechanism, the above results indicate that these asymmetrically modified graphene sheets could find uses in many novel optoelectronic nanodevices.

Owing to the highly generic nature of the plasma technique, together with the versatile  $\pi$ - $\pi$  stacking interaction between the pyrene-grafted entities and graphene surface, the methodology developed in this study could be regarded as a general approach toward the fabrication of multidimensional and multifunctional integrated graphene sheets with molecular-level control. Furthermore, the patterned and nonpatterned asymmetrical functionalization concepts reported herein are applicable to graphitic films with more than one graphene sheet and even many other nongraphitic films. Thus, we believe that the novel concepts and interesting optoelectronic characteristics demonstrated will have great impact on both fundamental and applied research in the field of materials science and engineering.

Received: February 22, 2011

Revised: April 11, 2011

Published online: June 6, 2011

**Keywords:** diodes · graphene · nanoparticles · photophysics · surface chemistry

- [1] a) S. Stankovich, D. A. Dikin, G. H. B. Dommett, K. M. Kohlhaas, E. J. Zimney, E. A. Stach, R. D. Piner, S. T. Nyugen, R. S. Ruoff, *Nature* **2006**, *442*, 282–286; b) K. S. Novoselov, A. K. Geim, S. V. Morozov, D. Jiang, Y. Zhang, S. V. Dubonos, I. V. Grigorieva, A. A. Firsov, *Science* **2004**, *306*, 666–669; c) X. Wang, L. J. Zhi, K. Mullen, *Nano Lett.* **2008**, *8*, 323–327; d) S. Gilje, H. Song, M. Wang, K. L. Wang, R. B. Kaner, *Nano Lett.* **2007**, *7*, 3394–3398; e) G. Eda, G. Fanchini, M. Chhowalla, *Nat. Nanotechnol.* **2008**, *3*, 270–274; f) Z. Liu, Q. Liu, Y. Huang, Y. Ma, S. Yin, X. Zhang, Y. Chen, W. Sun, Y. Chen, *Adv. Mater.* **2008**, *20*, 3924–3930; g) X. Li, X. Wang, L. Zhang, S. Lee, H. Dai, *Science* **2008**, *319*, 1229–1232; h) X. Li, G. Zhang, X. Bai, X. Sun, X. Wang, E. Wang, H. Dai, *Nat. Nanotechnol.* **2008**, *3*, 538–542; i) E. Yoo, J. Kim, E. Hosono, H. S. Zhou, T. Kudo, I. Honma, *Nano Lett.* **2008**, *8*, 2277–2282; j) M. D. Stoller, S. Park, Y. Zhu, J. An, R. S. Ruoff, *Nano Lett.* **2008**, *8*, 3498–3502.
- [2] a) D. Yu, L. Dai, *Appl. Phys. Lett.* **2010**, *96*, 143107; b) L. Qu, Y. Liu, J. Baek, L. Dai, *ACS Nano* **2010**, *4*, 1321–1326; c) D. Yu, L. Dai, *J. Phys. Chem. Lett.* **2010**, *1*, 467–470; d) Y. Liu, D. Yu, C. Zeng, Z. Miao, L. Dai, *Langmuir* **2010**, *26*, 6158–6160; e) X. Xie, L. Qu, C. Zhou, Y. Li, J. Zhu, H. Bai, G. Shi, L. Dai, *ACS Nano* **2010**, *4*, 6050–6054; f) C. Guo, H. Yang, Z. Sheng, Z. Lu, Q. Song, C. M. Li, *Angew. Chem.* **2010**, *122*, 3078–3081; *Angew. Chem. Int. Ed.* **2010**, *49*, 3014–3017; g) C. X. Guo, X. T. Zheng, Z. S. Lu, X. W. Lou, C. M. Li, *Adv. Mater.* **2010**, *22*, 5164–5167; h) C. X. Guo, Z. S. Lu, Y. Lei, C. M. Li, *Electrochem. Commun.* **2010**, *12*, 1237–1240.
- [3] a) S. Park, R. S. Ruoff, *Nat. Nanotechnol.* **2009**, *4*, 217–224; b) S. Niyogi, E. Bekyarova, M. E. Itkis, J. L. McWilliams, M. A. Hamon, R. C. Haddon, *J. Am. Chem. Soc.* **2006**, *128*, 7720–7721; c) D. Li, M. B. Müller, S. Gilje, R. B. Kaner, G. G. Wallace, *Nat. Nanotechnol.* **2008**, *3*, 101–105; d) Y. Xu, H. Bai, G. Lu, C. Li, G. Q. Shi, *J. Am. Chem. Soc.* **2008**, *130*, 5856–5857.
- [4] a) D. R. Dreyer, S. Park, C. W. Bielawski, R. S. Ruoff, *Chem. Soc. Rev.* **2010**, *39*, 228–240; b) K. P. Loh, Q. Bao, P. K. Ang, J. Yang, *J. Mater. Chem.* **2010**, *20*, 2277–2289.
- [5] a) K. M. Lee, L. Li, L. Dai, *J. Am. Chem. Soc.* **2005**, *127*, 4122–4123; b) M. Burghard, *Small* **2005**, *1*, 1148–1150.
- [6] a) L. Qu, L. Dai, *Chem. Commun.* **2007**, 3859–3861; b) Q. Peng, L. Qu, L. Dai, K. Park, R. Vaia, *ACS Nano* **2008**, *2*, 1833–1840; c) P. He, L. Dai, *Chem. Commun.* **2004**, 348–349.
- [7] F. Vietmeyer, B. Seger, P. V. Kamat, *Adv. Mater.* **2007**, *19*, 2935–2940.
- [8] Y. Ou, M. H. Huang, *J. Phys. Chem. B* **2006**, *110*, 2031–2036.
- [9] B. G. Burke, T. J. Herlihy, Jr., A. B. Spisak, K. A. Williams, *Nanotechnology* **2008**, *19*, 215301.
- [10] V. C. Tung, J. H. Huang, I. Tevis, F. Kim, J. Kim, C. W. Chu, S. I. Stupp, J. Huang, *J. Am. Chem. Soc.* **2011**, *133*, 4940–4947.
- [11] J. Liu, X. Li, L. Dai, *Adv. Mater.* **2006**, *18*, 1740–1744.
- [12] K. Mohanta, A. J. Pal, *Nanotechnology* **2009**, *20*, 185203.
- [13] A. B. Kaiser, C. Gómez-Navarro, R. S. Sundaram, M. Burghard, K. Kern, *Nano Lett.* **2009**, *9*, 1787–1792.
- [14] a) J. Kong, H. J. Dai, *J. Phys. Chem. B* **2001**, *105*, 2890–2893; b) J. Du, L. Fu, Z. Liu, B. Han, Z. Li, Y. Liu, Z. Sun, D. Zhu, *J. Phys. Chem. B* **2005**, *109*, 12772–12776; c) K. Mohanta, S. K. Batabyal, A. J. Pal, *Chem. Mater.* **2007**, *19*, 3662–3666.
- [15] a) C. Lin, B. Chu, G. Tobias, S. Sahakalkan, S. Roth, M. Green, S. Chen, *Nanotechnology* **2009**, *20*, 105703; b) G. D. Sharma, R. Kumara, S. K. Sharma, M. S. Royb, *Sol. Energy Mater. Sol. Cells* **2006**, *90*, 933–943.
- [16] G. Eda, C. Mattevi, H. Yamaguchi, H. Kim, M. Chhowalla, *J. Phys. Chem. C* **2009**, *113*, 15768–15771.